Nanoscale

Accepted Manuscript

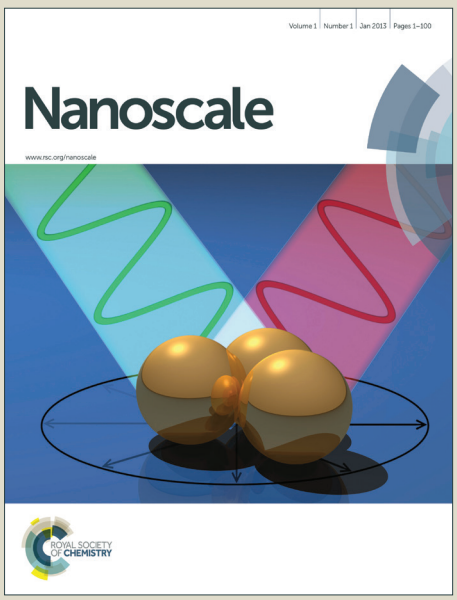

ROYAL SOCIETY OF CHEMISTRY

www.rsc.org/nanoscale

Cite this: DOI: 10.1039/c0xx00000x

www.rsc.org/xxxxxx

COMMUNICATION

MRI nanoprobes based on chemical exchange saturation transfer: Ln^{III} chelates anchored on the surface of mesoporous silica nanoparticles.

Giuseppe Ferrauto,[a] Fabio Carniato,[b] Lorenzo Tei,[b] He Hu,[a] Silvio Aime,*[a] and Mauro Botta*[b]

Received (in XXX, XXX) Xth XXXXXXXXX 20XX, Accepted Xth XXXXXXXXX 20XX
DOI: 10.1039/b000000x

The formation of ternary complexes between neutral Ln^{III}-DO3A chelates anchored on MCM-41 mesoporous silica nanoparticles (MSNs) and silanol groups on the surface allows to obtain highly efficient chemical exchange saturation transfer (CEST) MRI nanoprobes. These new probes achieve an excellent sensitivity in the μM range (per Ln^{III} ion), significantly greater than for other paramagnetic CEST nanosystems such as dendrimers or micelles and three orders of magnitude higher than that of the corresponding molecular agents.

Chemical Exchange Saturation Transfer (CEST) agents are an innovative class of contrast enhancement agents (CAs) for Magnetic Resonance Imaging (MRI).[1-2] They represent an attractive alternative to the commonly used T_1- and T_2- relaxation agents owing to their distinctive property to generate a frequency-encoded contrast. In fact, they can be switched *on* and *off* "at will", applying or not a rf pulse that saturates the resonances of exchanging protons. The saturated spins of the CEST probe are transferred to bulk water protons via chemical exchange thus generating a change in signal intensity (contrast) detectable in the ^{1}H-MR image. One of the main advantages relies on the possibility of visualizing more than one CEST probe simultaneously in the same voxel by simply changing the rf offset (Multicolor MRI).[3-4]

Various mechanisms of chemical exchange have been considered in the design of CEST agents, such as the proton exchange (*e.g.* the –OH proton in LnHPDO3A complexes), the molecular exchange (*e.g.* the water molecule in Ln-dotamgly complexes) or the compartment exchange (*e.g.* lipoCEST or erythoCEST).[5-8] However, just as for T_1 MR CAs, also for the CEST agents the limited sensitivity has emerged as a critical factor. Hence, nanosized systems containing a large number of mobile protons (including those paramagnetically shifted) have been designed to improve the sensitivity threshold. These include micelles or liposomes,[9] apoferritin,[10] virus nanoparticles[11] and perfluorocarbon droplets[12] loaded with paramagnetic agents. Recently, organo-modified mesoporous silica nanoparticles (MSNs) have met with considerable interest for biomedical applications thanks to a series of favourable properties: uniform mesopores, enhanced surface area, high chemical and thermal stability, easy chemical functionalization and good biocompatibility.[13] A number of Gd^{III}-complexes have been immobilized on nanosized (20-80 nm) MSNs and the chemical influence of the porous support on their magnetic properties has been extensively investigated.[14,15] Optimal MRI efficiency as T_1 agents (relaxivity, r_{1p}) was found by selectively anchoring macrocyclic GdDOTA-like complexes on the external surface of MSNs (r_{1p} of *ca.* 80 $mM^{-1}s^{-1}$ per Gd; 0.47 T and 37°C).[16]

The idea behind this work is to create, on the silica surface, ternary complexes between anchored LnDO3A and surface silanol moieties, *i.e.* to mimic the CEST properties of Ln-HPDO3A complexes where coordinating -OH functionality is the source of exchangeable protons.[17] The use of LnDO3A relies on two considerations: i) GdDO3A complex features two water molecules in the inner coordination sphere (q = 2) that can be easily displaced by coordinating anions;[18] ii) the relaxivity of a derivative of GdDO3A anchored to the surface of MCM-41 nanoparticles functionalized with $-NH_2/NH_3^+$ groups has been recently found to be unexpectedly low (r_{1p} = 14.6 $mM^{-1}s^{-1}$; 0.47 T and 37°C).[15] This finding can be explained on the basis of the displacement of one coordinated water molecule from the anchored GdDO3A chelates by the silanol groups present on the MSNs surface. The interaction reduces the accessibility of the solvent molecules to the paramagnetic centre, thus limiting the relaxivity. On this basis, we surmise that paramagnetic LnDO3A anchored onto mesoporous silica surface (LnDO3A-MCM-41) may act as CEST agent by exploiting the dipolar interaction with proximate OH groups (Fig. 1).

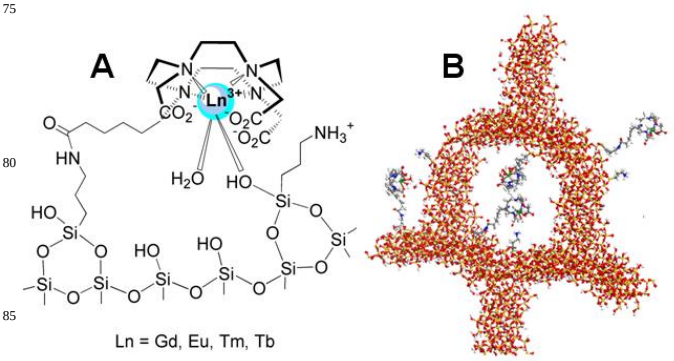

Figure 1. Schematic representation of: a) the interaction between LnDO3A-like chelates and the surface of the organo-modified MCM-41; B) Ln^{III} chelates anchored on the organo-modified mesoporous silica nanoparticles.

Interestingly, the idea of exploiting the silica surface to affect the proton exchange rate has been recently pursued by Sherry and co-workers by anchoring EuDOTA-Gly$_4$.[19] They aimed at slowing down the exchange rate of the coordinated water molecule but the net result was the complete removal of the water molecules following the interaction of the complex with the silica surface.

In this work, nanosized MCM-41 with particle sizes in the range 20–50 nm (by TEM analysis) and hydrodynamic diameter centred to *ca.* 100 nm (evaluated by DLS analysis) were prepared and functionalized with amino groups. Then, neutral Ln^{III} (where Ln = Eu, Tm, Tb, Gd) complexes of a DO3A derivative bearing a hexanoic acid pendant group were anchored onto the MCM-41 silica surface by reaction between the free carboxylic group of the chelates and the $–NH_2$ functionalities of the MSNs, following the synthetic approach previously described (Fig. 1).[15] The physico-chemical properties of the labelled silica nanoparticles were determined by high resolution TEM microscopy, IR spectroscopy, and N_2 physisorption measurements (see ESI for details) with results in agreement with published data.[15] The data reported in Table 1 show the amount of Ln^{III} in the final hybrid materials, measured by ICP-MS technique, and the loading of LnDO3A chelates for each MSN nanoparticle, estimated by adapting a method reported in the literature.[20] Data obtained by thermogravimetric analysis suggest that the number of Si-OH groups present on the surface of the functionalized silica is *ca.* two per nm^2.

Table 1. Quantification of the chelates anchored on the MCM-41 surface.

	EuDO3A	TmDO3A	TbDO3A	GdDO3A
Ln^{III} concentration (mmol/g)	0.12	0.15	0.05	0.04
Number of Ln^{III} chelates per particle	820	1000	350	250
Saturation offset (ppm)	5.5	7.5	15	n.a.

The CEST properties were evaluated at 7.1 T, 21 °C, pH 7 by acquiring Z-spectra on a Bruker 300 MHz Spectrometer equipped with a micro-imaging probe. The RARE sequence was preceded by the pre-saturation scheme that consists in a continuous rectangular block pulse (B_1 = 24μT, irradiation time 2 sec).

The ST%-spectra of the four LnDO3A-MCM-41 materials and the control silica (*i.e.* without anchored complexes) are shown in Fig. 2. The chemical shift varies with the nature of the lanthanide ion assuming the values of 5.5, 7.5 and 15 for Eu-, Tm- and Tb-silica, respectively. In the case of control silica, no CEST effect is detected, given the close proximity of the chemical shift values of water and hydroxyl protons in the absence of a paramagnetic centre. Likewise, by loading Gd-complexes on the silica surface, no CEST effect is observed as the Gd^{III} ion does not induce a paramagnetic shift to the –OH proton signal through dipolar interaction (C^J=0 for Gd^{III}). As expected, the dipolar shift increases moving from Eu- to Tb-complex but, unexpectedly, it decreases to *ca.* 7.5 ppm for TmDO3A-MCM-41. The observed behaviour may be accounted in terms of a changeover of the hydration number *q* of LnDO3A chelates from *ca.* 2 to *ca.* 1 across the Ln series. A lower hydration state for the Tm^{III}-chelate results in a hindrance of the interaction with the -OH groups on the silica surface and therefore in an increased average distance of the paramagnetic ion which attenuates the efficacy of the dipolar coupling. The ST_{maps} obtained by irradiating at different offsets, reported in Fig. 3, highlight the possibility to distinguish among the phantoms containing the different LnDO3A-MCM-41 nanoparticles. Therefore, such system can be used for multicolour MR imaging.

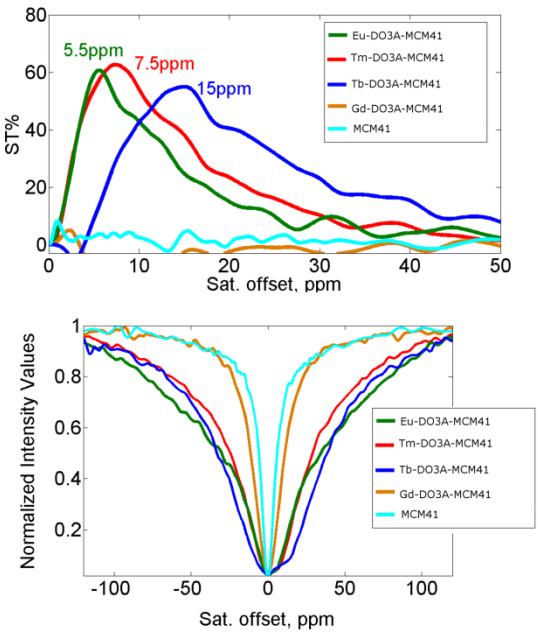

Figure 2. Comparison between ST- (above) and Z- (below) spectra of different LnDO3A-MCM-41 nanoparticles.

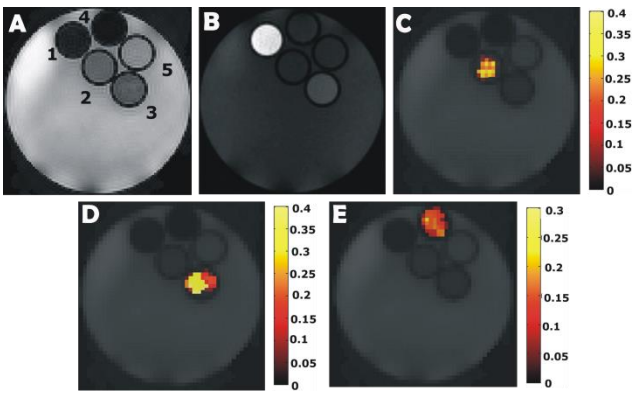

Figure 3. T_{2w} (A), T_{1w} (B), ST_{map} at 5.5 ppm (C), ST_{map} at 7.5 ppm (D) and ST_{map} at 15 ppm (E) of a phantom made by 5 glass capillaries containing: 1) GdDO3A-MCM-41, 2) EuDO3A-MCM-41, 3) TmDO3A-MCM-41, 4) TbDO3A-MCM-41, 5) unlabelled MCM-41.

Moreover, the detection threshold for Eu- Tb- and TmDO3A-MCM-41 silica has been assessed by progressive dilution of silica suspensions in saline phosphate buffer (PBS) solution. As shown

for TbDO3A-MCM-41 (Fig. 4), the ST% is higher than 5% (our arbitrary choice as threshold for visualization) up to a silica concentration of 1.25 mg/mL, that corresponds to a Tb^{III} concentration of *ca.* 70 μM. Similar results were obtained for Eu- and TmDO3A-MCM-41 (see ESI, Fig. S8 and S9).

The pH and temperature dependences of TbDO3A-MCM-41 were also assessed showing that the ST% effect does not substantially change in the 6.0-8.5 pH range and 29-45 °C temperature range (Fig. S10). However, the ST% effect rapidly diminishes below pH 6 probably due either to an increased rate of exchange of the pool of protons interacting with the Ln-chelates or to a substantial alteration of the silica surface and thus to a change in the interaction between the silanol groups and the LnDO3A complexes, both promoted by low pH values.

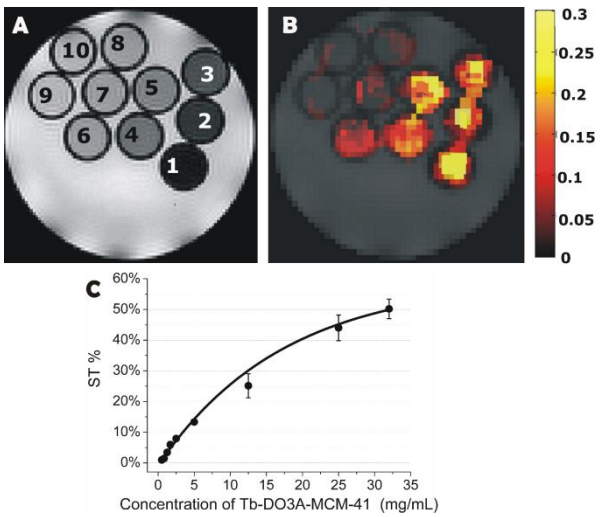

Figure 4. T_{2w} image (A) and ST image at 14 ppm (B) of TbDO3A-MCM-41 at variable concentration (1 = 25 mg/mL, 2 = 12.5 mg/mL, 3 = 5 mg/mL, 4 = 2.5 mg/mL, 5 = 1.7 mg/mL, 6 = 1.25 mg/mL, 7 = 0.83 mg/mL, 8 = 0.5 mg/mL, 9 = 0.25 mg/mL, 10 = 0 mg/mL); (C) ST% vs. Concentration of TbDO3A-MCM-41.

In principle, the LnDO3A-MCM-41 systems can be considered as the "particulate version" of LnHPDO3A para-CEST agents.[4,17] In fact, though LnHPDO3A present higher dipolar shifts than those found for the LnDO3A-SiO_2 systems, the CEST sensitivity of the latter ones appears definitively much higher than that reported for molecular LnHPDO3A complexes. These findings led us to surmise that the higher CEST sensitivity and the smaller dipolar shift of the –OH moieties in LnDO3A anchored on silica surface are the results of the reversible and multiple interaction of the metal ion in the LnDO3A cage with a number of silanol groups in the neighbourhood of the anchoring site on the particle surface. Alternatively, the smaller dipolar shift could be attributed to a weaker interaction of the silanol groups, partially hindered in accessing the coordination cage; in addition, the larger CEST efficiency might be associated with an increased prototropic exchange rate.

Conclusions

In summary, novel nanoCEST agents based on LnDO3A derivatives anchored on MCM-41 mesoporous silica NPs are reported to successfully shift the surface silanol protons. TbDO3A is the most efficient among the LnDO3A chelates studied (Ln = Eu, Tm, Tb, Gd) showing a larger shift and an excellent sensitivity down to the μM range. The sensitivity threshold is excellent, being not only dramatically lower than the corresponding monomeric Ln-HPDO3A complexes but also significantly enhanced with respect to that reported for other paramagnetic nanosystems such as dendrimers and micelles. The sensitivity is comparable to that of Ln-complexes encapsulated in the inner core of liposomes while being associated with markedly lower size (Fig. 5).

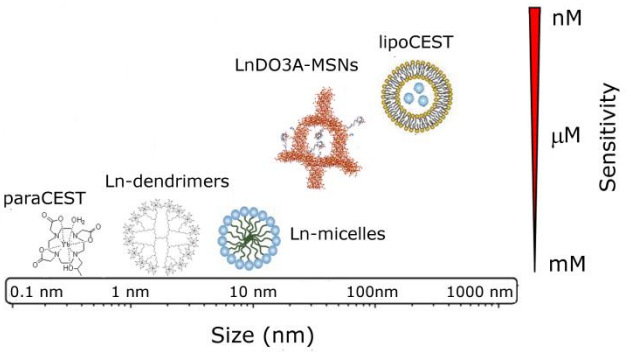

Figure 5. Comparison among different nanosized CEST probes in term of size and sensitivity. The sensitivity is related to the minimum concentration of Ln-complexes needed to obtain a detectable Saturation Transfer effect (ST% >5%).

Finally, considering that the three domains of MSNs (silica framework, internal pore walls, and outer surface) can be easily and independently functionalized, MSNs represent an optimal scaffold for multimodal probes or for drug delivery and controlled release. In light of these considerations, the reported nanoCEST probe appears very promising for future in vivo use in multimodal imaging or in theranostic applications and a good alternative to the already reported nanosized CEST probes.

Acknowledgements

The financial support of the "Compagnia di San Paolo" (CSP-2012, NANOPROGLY Project) is gratefully acknowledged. H.H. thanks the Marie Curie fellowship (FP7-PEOPLE-2011-IIF-UHMSNMRI).

Notes and references

[a]*Department of Molecular Biotechnology and Health Sciences, Molecular Imaging Center, University of Torino, Via Nizza, 52, 10126, Torino, Italy.*
[b]*Dipartimento di Scienze e Innovazione Tecnologica, Università del Piemonte Orientale "Amedeo Avogadro" Viale T. Michel 11, 15121, Alessandria, Italy.*

† Electronic Supplementary Information (ESI) available: Synthesis and characterization of the materials; Z- and ST-spectra of all materials; sensitivity threshold for TmDO3A-MCM-41; pH and temperature dependence of ST% for TbDO3A-MCM-41. See DOI: 10.1039/b000000x/

1 A.D Sherry, M. Woods, *Annu. Rev. Biomed. Eng.*, 2008, **10**, 391-411.
2 E. Terreno, D. Delli Castelli, S. Aime, *Contrast Media Mol. Imaging*, 2010, **5**, 78–98.
3 M. T. McMahon, A. A. Gilad, M. A. DeLiso, S. M. Berman, J. W. Bulte, P. C. van Zijl, *Magn Reson Med.*, 2008, **60**, 803-812.
4 G. Ferrauto, D. Delli Castelli, E. Terreno, S. Aime, *Magn. Reson. Med.*, 2013, **69**, 1703-1711.
5 P. C. van Zijl, N. N Yadav, *Magn. Reson. Med.*, 2011, **65**, 927-948.
6 D. Delli Castelli, E. Terreno, D. Longo, S. Aime, *NMR Biomed.*, 2013, **26**, 839-849.
7 Aime S, D. Delli Castelli, E. Terreno, *Methods Enzymol.*, 2009, **464**, 193-210.
8 G. Ferrauto, D. Delli Castelli, E. Di Gregorio, S. Langereis, D. Burdinski, H. Grüll, E. Terreno, S. Aime, *J. Am. Chem. Soc.*, 2014, **136**, 638-641.
9. S. Aime, D. Delli Castelli, S. Geninatti Crich, E. Gianolio, E. Terreno, *Acc. Chem. Res.*, 2009, **42**, 822-831; S. Zhang, K. Zhou, G. Huang, M Takahashi, A. D. Sherry, J. Gao, *Chem Commun*, 2013, **49**, 6418-6420.
10. O. Vasalatiy, P. Zhao, S. Zhang, S. Aime, A. D. Sherry, *Contrast Media Mol. Imaging*, 2006, **1**, 10–14.
11. O. Vasalatiy, R. D. Gerard, P. Zhao, X. K.Sun, A. D. Sherry, *Bioconjug. Chem.*, 2008, **19**, 598–606.
12. P. M. Winter, K. J. Cai, J. Chen, C. R. Adair, G. E. Kiefer, P. S. Athey, P. J. Gaffney, C. E. Buff, J. D. Robertson, S. D. Caruthers, S. A. Wickline, G. M. Lanza, *Magn. Reson. Med.*, 2006, **56**, 1384–1388.
13. Y. Chen, H. Chen, J. Shi, *Adv. Mater.* 2013, **25**, 3144–3176.
14. F. Carniato, L. Tei, W. Dastrù, L. Marchese, M. Botta, *Chem. Commun.*, 2009, 1246–1248.
15. F. Carniato, L. Tei, M. Cossi, L. Marchese, M. Botta, *Chem. Eur. J.*, 2010, **16**, 10727–10734.
16. F. Carniato, L. Tei, A. Arrais, L. Marchese, M. Botta, *Chem. Eur. J.*, 2013, **19**, 1421–1428.
17. D. Delli Castelli, E. Terreno, S. Aime. *Angew. Chem. Int. Ed. Engl.*, 2011, **50**, 1798-800.
18. S. Aime, M. Botta, S. G. Crich, G. B. Giovenzana, R. Pagliarin, M. Sisti, E. Terreno, *Magn. Reson. Chem.*, 1998, **36**, S200.
19. O. M. Evbuomwan, M. E. Merritt, G. Kiefer, A. D. Sherry, *Contrast Media Mol. Imaging*, 2012, **7**, 19–25.
20. W. J. Rieter, J. S. Kim, K. M. L. Taylor, H. An, W. Lin, T. Tarrant, W. Lin, *Angew. Chem. Int. Ed.*, 2007, **46**, 3680.